2019

Controlling the magnetocrystalline anisotropy of E-Fe2O3

Imran Ahamed

Ralph Skomski

Arti Kashyap

Controlling the magnetocrystalline anisotropy of ε-Fe_2O_3

Cite as: AIP Advances **9**, 035231 (2019); https://doi.org/10.1063/1.5080144
Submitted: 05 November 2018 . Accepted: 21 January 2019 . Published Online: 18 March 2019

Imran Ahamed, Ralph Skomski, and Arti Kashyap

Controlling the magnetocrystalline anisotropy of ε-Fe_2O_3

Cite as: AIP Advances 9, 035231 (2019); doi: 10.1063/1.5080144
Presented: 16 January 2019 • Submitted: 5 November 2018 •
Accepted: 21 January 2019 • Published Online: 18 March 2019

Imran Ahamed,[1,a)] Ralph Skomski,[2] and Arti Kashyap[1]

AFFILIATIONS

[1]School of Basic Sciences, Indian Institute of Technology, Mandi, HP 175001, India
[2]Nebraska Center for Materials and Nanoscience & Department of Physics and Astronomy, University of Nebraska, Lincoln, Nebraska 68588, USA

Note: This paper was presented at the 2019 Joint MMM-Intermag Conference.
[a)]Imran Ahamed. **Mail to:** iahamed89@gmail.com

ABSTRACT

The magnetocrystalline anisotropy of pristine and Co-substituted ε-Fe_2O_3 is investigated by density functional calculations. The epsilon-iron oxide is the only polymorph of Fe_2O_3 magnetoelectric in its antiferromagnetic ground states other crystalline forms being α-Fe_2O_3 (hematite), β-Fe_2O_3, and γ-Fe_2O_3 (maghemite). The magnetizations of the four iron sublattices are antiferromagnetically aligned with slightly different magnetic moments resulting in a ferrimagnetic structure. Compared to the naturally occurring hematite and maghemite, bulk ε-Fe_2O_3 is difficult to prepare, but ε-Fe_2O_3 nanomaterials of different geometries and feature sizes have been fabricated. A coercivity of 20 kOe [2 T] was reported in nanocomposites of ε-Fe_2O_3, and an upper bound for the magnetic anisotropy constant K at a low temperature of ε-Fe_2O_3 is previously measured to be 0.1 MJ/m^3. In the Co-substituted oxides, one octahedral or tetrahedral Fe atom per unit cell has been replaced by Co. The cobalt substitution substantially enhances magnetization and anisotropy.

I. INTRODUCTION

Iron sesquioxide, Fe_2O_3, exists in form of several polymorphs: the common α-Fe_2O_3 (hematite), γ-Fe_2O_3 (maghemite) and the rare polymorphs β-Fe_2O_3 and ε-Fe_2O_3.[1] Epsilon-Fe_2O_3 was first reported in 1934 by Forestier and Guiot-Guillain. Later, Schrader and Büttner[2] in 1963 and Trautmann and Forestier in 1965 studied its magnetic properties, especially its anisotropy.[3] ε-Fe_2O_3 has been naturally found in the ancient Chinese pottery as patterns on the pots,[4] in archeological sites around Europe,[5,6] and very recently in young basaltic rocks.[7] Very recently, the mineral Luogufengite[8] has been identified by Xu *et al.*,[7] as being Al-containing ε-Fe_2O_3. The laboratory-synthesized ε-Fe_2O_3 and the mineral have the same structure and magnetic properties. The laboratory-prepared sample and the natural mineral have the lattice parameters as a = 5.095, b = 8.789 and c = 9.437 Å,[9] and a = 5.0647, b = 8.7131, c = 9.3842 Å,[7] respectively.

The crystal structure of ε-Fe_2O_3 is orthorhombic, has the space group $Pna2_1$, and contains 8 formula units per unit cell.[9] Figure 1 shows that the unit cell contains four different Fe sites, namely two distorted octahedral sites (Fe_A and Fe_B), a regular octahedral site (Fe_C) and a regular tetrahedral site (Fe_D). The interatomic exchange interaction is of A-type antiferromagnetic, with the spin arrangement of β, α, α, β for the Fe_A, Fe_B, Fe_C, Fe_D atoms, respectively. The spin structure of this system is not fully understood and it is reported as collinear[10–12] and noncollinear[1,9] ferrimagnetic. Recently, Xu *et al.*,[13] predicted spin frustration of the Fe_D sites, resulting in a noncollinear spin structure with the energy of 60 meV/f.u. lower than that of the experimentally suggested collinear spin structure. The ferrimagnetism in the bulk is due to the uncompensated moments of regular octahedral (Fe_C) and regular tetrahedral (Fe_D), both arranged in antiferromagnetic order and the moments of the two distorted octahedral being equal cancels each other.[14]

The oxide is magnetoelectric[15] with a switchable ferroelectric polarization[13] and ferrimagnetic with a Curie temperature of 510 K.[10] Nanoparticles of ε-Fe_2O_3 are reported to have a high coercivity of about 20 kOe [2 T],[1,10,16] but thin-film coercivities

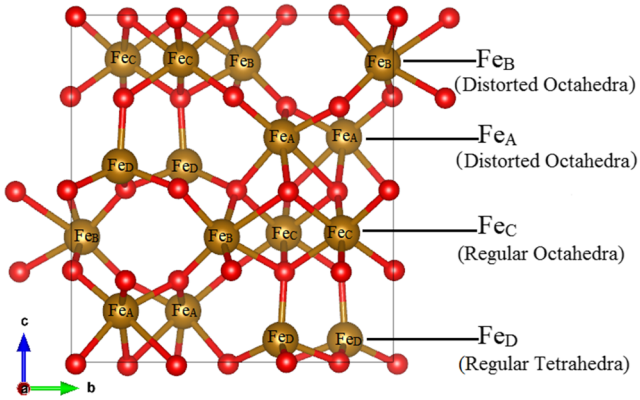

FIG. 1. The unit cell of ε-Fe_2O_3. (Red atoms are oxygen and Fe in different coordination in different colors).

are lower.[17,18] An upper bound to the low-temperature magnetic anisotropy constant K of ε-Fe_2O_3 is previously measured to be 0.1 MJ/m^3.[19] Since ε-Fe_2O_3 is an intermediate phase of hematite (α-Fe_2O_3) and maghemite (γ-Fe_2O_3),[20,21] the structure of its unit cell has Fe-atoms of both coordination as well.

There have been experimental attempts to further enhance and improve the coercivity of this particular phase of Fe_2O_3 by substitution of Fe-atoms on different sites by non-magnetic atoms such as indium, aluminum, gallium, and rhodium, in different concentrations. Namai *et al.*[22] chemically prepared a series of Rh-substituted ε-Fe_2O_3 nanoparticles and obtained enhanced coercivities of 2.7 and 3.1 T for isotropic and crystallographically aligned nanoparticles, respectively. In this case, the Rh-atom occupies the Fe-atom at C-site. Ohkoshi *et al.*[21] prepared In-, Ga- and Al-substituted ε-Fe_2O_3, with various concentrations and substitutions taking place at every Fe-site and obtained a tunability of the coercivity. In Al-substituted ε-Fe_2O_3 ($Fe_{1.7}Al_{0.3}$), the Al atoms preferentially occupy the Fe_D sites[21,23] but reduces the coercivity.

In this work, we have studied the effect of Co substitution on different Fe sites. We have replaced a single A, C, and D type Fe atom per unit cell by Co and calculated the saturation magnetization (M_s), the effective magnetic anisotropy constant ($K_{effective}$) and the anisotropy field (H_A). Since the anisotropy field is the upper bound to the coercivity, the variation of H_A with the site substitution will give a good estimate of the coercivity of the system. We also identify the site-specific origin of the anisotropy change and compare the situation in ε-Fe_2O_3 with the anisotropy contribution in α-Fe_2O_3 and γ-Fe_2O_3.

II. METHOD

Density functional theory (DFT) based on the Vienna *ab-initio* simulation package (VASP)[24–26] was used for the calculation. The Perdew, Burke, and Ernzerhof (PBE)[27] functional was used to incorporate semi-local exchange-correlation effects. The DFT+U[28] formalism was implemented to account for the strongly correlated nature of the Fe 3*d* localized electrons. We took $U–J$ = 4 eV for ε-Fe_2O_3[11,29] a value commonly used for the hematite. For Co-substituted ε-Fe_2O_3, the value of U-J are 4 eV and 3.3 eV[29] for the 3*d*-states of Fe- and Co-atom, respectively. Projected Augmented Wave (PAW)[26] method-based potentials were used for Fe-, O-, and Co-atoms. The valence-electron configurations for the Fe-, O-, and Co-atoms were taken to be d^7s^1, s^2p^4, and d^8s^1, respectively. The electronic wave functions were represented by a plane-wave basis set with an energy cutoff of 530 eV. A Monkhorst-Pack[30] k-point mesh of 5 × 3 × 3 was used for one unit cell for structural optimization of the pristine bulk as well as of the Co-substituted ε-Fe_2O_3. A convergence criterion of 10^{-7} eV for electronic self-consistency and maximum forces of 0.005 eV/Å for each atom during structural optimization were chosen.

To calculate the effective magnetic anisotropy and the anisotropy field for the pristine as well Co-substituted ε-Fe_2O_3, we included the spin-orbit coupling as implemented in VASP by Kresse and Lebacq. A very dense Monkhorst-Pack k-point mesh of 15 × 9 × 9 was used to calculate the total energies for the magnetization directions fixed parallel to the x-, y-, and z-axes. Due to the orthorhombic nature of the crystal, there exists low symmetry and the lowest order anisotropy energy[31,32] is defined as

$$E = K_1 V \sin^2\theta + K_1' V \sin^2\theta \cos(2\Phi) \quad (1)$$

Using Eq. 1, the effective magnetic anisotropy constant was calculated using the formula

$$K_{eff} = (E_{first\ hard\ axis} - E_{easy\ aixs})/V \quad (2)$$

which yields the anisotropy field

$$H_A = 2K_{eff}/\mu_0 M_s \quad (3)$$

where E is the total ground state energy of the system, V is the volume of the unit cell of bulk ε-Fe_2O_3, μ_0 is the permeability of free space and M_s is the saturation magnetization of the bulk ε-Fe_2O_3.

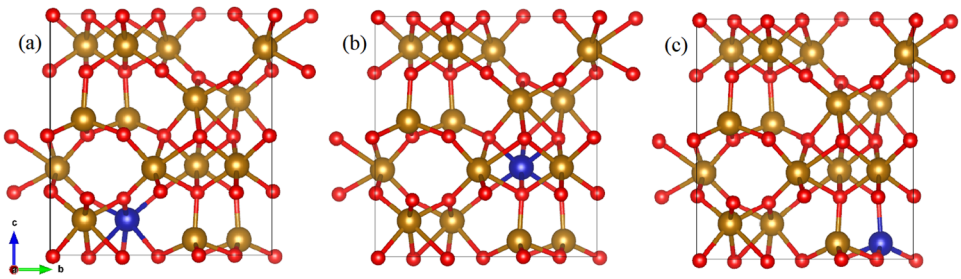

FIG. 2. Co-substitution on Fe in ε-Fe_2O_3 at sites: (a) Fe_A, (b) Fe_C, and (c) Fe_D. (The red, brown, and blue atoms are O, Fe, and Co, respectively).

III. RESULTS AND DISCUSSION

Our DFT optimized lattice parameters obtained for ε-Fe_2O_3 are as a = 5.125, b = 8.854 and c = 9.563 Å,[33,34] which is in agreement with the experimental lattice parameters of Sect. I. Our calculated electronic structure yields an energy band-gap of 1.9 eV.[33,34] Figure 2 shows the unit-cell structures of the Co-substituted ε-Fe_2O_3. For the Co-substitution, we kept the volume of the unit cell constant and only the ionic positions were relaxed. Taking into account the non-uniaxial character of the orthorhombic lattice,[31] the total energies were calculated for magnetization directions along the three principal axes.

The saturation magnetization (M_s), effective magnetic anisotropy constant (K_{eff}) and anisotropy field (H_A) for the Co-free and Co-substituted oxides are listed in Table I. The table shows that the K_{eff} of the pristine bulk ε-Fe_2O_3 is comparable to the previously measured K value of 0.1 MJ/m^3,[19] which was the upper cutoff of anisotropy constant. Both theory and experiment yield a substantial anisotropy increase due to transition-metal substitution. One reason is the anisotropy of the starting compound, which is unusually low for a noncubic compound. The anisotropy constants of the Co-substituted oxides are typical for noncubic materials (several 0.1 MJ/m^3). The anisotropy field, which provides an upper bound to the coercivity, is an order of magnitude higher than the experimentally reported[1,10,16] coercivity. As explained in Ref. 32, such a difference is not unusual and means that the coercivity mechanism deviates from coherent rotation due to real-structure effects.

On all three Fe sites (distorted octahedra, regular octahedra, and regular tetrahedra), the Co atoms keep interacting antiferromagnetically, maintaining the ferrimagnetic order but enhancing the total magnetization (Table I). Among the doped systems, the substitution at the tetrahedral site does not contribute to the enhancement of the anisotropy field, because the anisotropy and magnetization changes cancel each other. Among the two octahedrals, the distorted one has the bigger effect on both K_{eff} and on H_A. The distorted octahedral is not present in the structures of hematite and maghemite; it occurs in the ε-Fe_2O_3 crystal structure only, where it has a big effect on anisotropy and on the coercivity.

TABLE I. Saturation magnetization, effective magnetic anisotropy and anisotropy field of pristine and Co-substituted unit cell.

System	M_s per unit cell (kA/m)	K_{eff} (MJ/m^3)	HA (T)
Pristine bulk	2.95	0.034	23.06
Co substitution at distorted octahedra (A-site)	24.32	0.769	63.27
Co substitution at regular octahedra (C-site)	18.72	0.444	47.46
Co substitution at regular tetrahedra (D-site)	23.61	0.273	23.13

IV. CONCLUSIONS

In summary, we have studied the site substitution effect of Co on the magnetization, magnetic anisotropy, and anisotropy field of ε-Fe_2O_3. The distorted octahedron which is exclusive to the ε-Fe_2O_3 crystal structure and not found in hematite or maghemite, are important for the understanding of the anisotropy of the oxide. On Co substitution, they yield a disproportional contribution to anisotropy and coercivity. On the other hand, if the substitution takes places by a d-states element, such as Rh and Co, the magnetic anisotropy constant as well as the coercivity increases.

ACKNOWLEDGMENTS

Thanks are due to A. Ullah for help in details. This work is supported by Nano Mission, DST, India (SR/NM/NS-1198/2013, IA, AK) and by DOE/BES (DE-FG02-04ER46152, RS).

REFERENCES

[1] R. Zboril, M. Mashlan, and D. Petridis, Chem. Mater. **14**, 969 (2002).
[2] R. Schrader and G. Büttner, Zeitschrift für Anorganische und Allgemeine Chemie **320**, 220 (1963).
[3] I. Dézsi and J. M. D. Coey, Physica Status Solidi (A) **15**, 681 (1973).
[4] C. Dejoie, P. Sciau, W. Li, L. Noé, A. Mehta, K. Chen, H. Luo, M. Kunz, N. Tamura, and Z. Liu, Scientific Reports **4**, 4941 (2014).
[5] G. McIntosh, M. Kovacheva, G. Catanzariti, M. L. Osete, and L. Casas, Geophysical Research Letters **34**, https://doi.org/10.1029/2007gl031168 (2007).
[6] G. McIntosh, M. Kovacheva, G. Catanzariti, F. Donadini, and M. L. O. Lopez, Geochemistry, Geophysics, Geosystems **12** (2011).
[7] H. Xu, S. Lee, and H. Xu, American Mineralogist **102**, 711 (2017).
[8] U. Hålenius, F. Hatert, M. Pasero, and S. J. Mills, Mineralogical Magazine **80**, 691 (2016).
[9] E. Tronc, C. Chanéac, and J. P. Jolivet, Journal of Solid State Chemistry **139**, 93 (1998).
[10] M. Popovici, M. Gich, D. Nižňanský, A. Roig, C. Savii, L. Casas, E. Molins, K. Zaveta, C. Enache, J. Sort, S. de Brion, G. Chouteau, and J. Nogués, Chem. Mater. **16**, 5542 (2004).
[11] M. Yoshikiyo, K. Yamada, A. Namai, and S. Ohkoshi, J. Phys. Chem. C **116**, 8688 (2012).
[12] J. Tucek, S. Ohkoshi, and R. Zboril, Appl. Phys. Lett. **99**, 253108 (2011).
[13] K. Xu, J. S. Feng, Z. P. Liu, and H. J. Xiang, Phys. Rev. Applied **9**, 044011 (2018).
[14] Y.-C. Tseng, N. M. Souza-Neto, D. Haskel, M. Gich, C. Frontera, A. Roig, M. van Veenendaal, and J. Nogués, Phys. Rev. B **79**, 094404 (2009).
[15] M. Gich, C. Frontera, A. Roig, J. Fontcuberta, E. Molins, N. Bellido, C. Simon, and C. Fleta, Nanotechnology **17**, 687 (2006).
[16] J. Jin, S. Ohkoshi, and K. Hashimoto, Advanced Materials **16**, 48 (2004).
[17] M. Gich, J. Gazquez, A. Roig, A. Crespi, J. Fontcuberta, J. C. Idrobo, S. J. Pennycook, M. Varela, V. Skumryev, and M. Varela, Appl. Phys. Lett. **96**, 112508 (2010).
[18] A. Tanskanen, O. Mustonen, and M. Karppinen, APL Materials **5**, 056104 (2017).
[19] M. Gich, A. Roig, C. Frontera, E. Molins, J. Sort, M. Popovici, G. Chouteau, D. Martín y Marero, and J. Nogués, Journal of Applied Physics **98**, 044307 (2005).
[20] Y. Ding, J. R. Morber, R. L. Snyder, and Z. L. Wang, Advanced Functional Materials **17**, 1172 (2007).
[21] S. Ohkoshi and H. Tokoro, BCSJ **86**, 897 (2013).
[22] A. Namai, M. Yoshikiyo, K. Yamada, S. Sakurai, T. Goto, T. Yoshida, T. Miyazaki, M. Nakajima, T. Suemoto, H. Tokoro, and S. Ohkoshi, Nature Communications **3**, 1035 (2012).
[23] T. Nasu, M. Yoshikiyo, H. Tokoro, A. Namai, and S. Ohkoshi, European Journal of Inorganic Chemistry **2017**, 530 (2017).

[24]G. Kresse and J. Furthmüller, Computational Materials Science **6**, 15 (1996).
[25]G. Kresse and J. Furthmüller, Phys. Rev. B **54**, 11169 (1996).
[26]G. Kresse and D. Joubert, Phys. Rev. B **59**, 1758 (1999).
[27]J. P. Perdew, K. Burke, and M. Ernzerhof, Phys. Rev. Lett. **77**, 3865 (1996).
[28]J. Hubbard, Proc. R. Soc. Lond. A **276**, 238 (1963).
[29]G. W. Mann, K. Lee, M. Cococcioni, B. Smit, and J. B. Neaton, The Journal of Chemical Physics **144**, 174104 (2016).
[30]H. J. Monkhorst and J. D. Pack, Phys. Rev. B **13**, 5188 (1976).
[31]R. Skomski, J. Phys.: Condens. Matter **15**, R841 (2003).
[32]R. Skomski, *Simple Models of Magnetism* (Oxford University Press, Oxford, New York, 2008).
[33]I. Ahamed, R. Pathak, R. Skomski, and A. Kashyap, AIP Advances **8**, 055815 (2017).
[34]I. Ahamed, K. Ulman, N. Seriani, R. Gebauer, and A. Kashyap, J. Chem. Phys. **148**, 214707 (2018).